ANNALS of Clinical and Translational Neurology
Open Access
ANA American Neurological Association since 1875

RESEARCH ARTICLE

7 Tesla MRI of Balo's concentric sclerosis versus multiple sclerosis lesions

Janina R. Behrens[1,2,3,a], Julia Wanner[1,2,3,a], Joseph Kuchling[1,2,3], Lennard Ostendorf[1,2,3], Lutz Harms[2,4], Klemens Ruprecht[1,2,4], Thoralf Niendorf[5,6,7], Sven Jarius[8], Brigitte Wildemann[8], René M. Gieß[1,2,3], Michael Scheel[1,2,3], Judith Bellmann-Strobl[1,2,3,6,7], Jens Wuerfel[1,9,11], Friedemann Paul[1,2,3,4,6,7,b] & Tim Sinnecker[1,9,10,b]

[1]Charité – Universitätsmedizin Berlin, Corporate Member of Freie Universität Berlin, Humboldt-Universität zu Berlin, and Berlin Institute of Health, NeuroCure Cluster of Excellence, NeuroCure Clinical Research Center, Berlin, Germany
[2]Charité – Universitätsmedizin Berlin, Corporate Member of Freie Universität Berlin, Department of Neurology, Humboldt-Universität zu Berlin, and Berlin Institute of Health, Berlin, Germany
[3]Berlin Institute of Health, Berlin,Germany
[4]Clinical and Experimental Multiple Sclerosis Research Center, Charite – Universitätsmedizin Berlin, Berlin, Germany
[5]Berlin Ultrahigh Field Facility, Max Delbrück Center for Molecular Medicine in the Helmholtz Association, Berlin, Germany
[6]Experimental and Clinical Research Center, Charite – Universitätsmedizin Berlin, Berlin, Germany
[7]Max Delbrück Center for Molecular Medicine, Berlin, Germany
[8]Molecular Neuroimmunology Group, Department of Neurology, University of Heidelberg, Heidelberg, Germany
[9]Medical Image Analysis Center (MIAC AG), Basel, Switzerland
[10]Department of Neurology, Universitätsspital Basel, Basel, Switzerland
[11]qbig, Department of Biomedical Engineering, University Basel, Basel, Switzerland

Correspondence
Friedemann Paul, NeuroCure Clinical Research Center, Charité – Universitätsmedizin Berlin, Charitéplatz 1, 10117 Berlin, Germany.
Tel: +49 (0)30 450 539 705; Fax: +49 (0)30 450 539 915;
E-mail: friedemann.paul@charite.de

Funding Information
No funding information provided.

Received: 20 December 2017; Revised: 18 March 2018; Accepted: 6 April 2018

Annals of Clinical and Translational Neurology **2018; 5(8): 900–912**

doi: 10.1002/acn3.572

[a]Equally contributing first authors.
[b]Equally contributing senior authors.

Abstract

Background: Baló's concentric sclerosis (BCS) is a rare condition characterized by concentrically layered white matter lesions. While its pathogenesis is unknown, hypoxia-induced tissue injury and chemotactic stimuli have been proposed as potential causes of BCS lesion formation. BCS has been suggested to be a variant of multiple sclerosis (MS). Here, we aimed to elucidate similarities and differences between BCS and MS by describing lesion morphology and localization in high-resolution 7 Tesla (7 T) magnetic resonance imaging (MRI) scans. **Methods**: Ten patients with Baló-type lesions underwent 7 T MRI, and 10 relapsing remitting MS patients served as controls. The 7 T MR imaging protocol included 3D T_1-weighted (T_1w) magnetization-prepared rapid gradient echo, 2D high spatial resolution T_2*-weighted (T_2*w) fast low-angle shot and susceptibility-weighted imaging. **Results**: Intralesional veins were visible in the center of all but one Baló-type lesion. Four Baló-type lesions displayed inhomogeneous intralesional T_2*w signal intensities, which are suggestive of microhemorrhages or small ectatic venules. Eight of 10 BCS patients presented with 97 additional lesions, 36 of which (37%) had a central vein. Lesions involving the cortical gray matter and the U-fibers were not detected in BCS patients. **Conclusion**: Our findings support the hypothesis that BCS and MS share common pathogenetic mechanisms but patients present with different lesion phenotypes.

Introduction

Prior to the availability of high-resolution magnetic resonance imaging (MRI), Baló's concentric sclerosis (BCS) was diagnosed by the presence of large, inflammatory lesions with concentric rings within the brain's white matter obtained via autopsy or biopsy.[1–3] BCS was believed to be a destructive focal neuroinflammatory condition and entailed a devastating prognosis.[1,4,5] With the increasing use of MRI, diagnosis of BCS is now generally based on radiographic findings and identified already early in the course of the disease.[1,4]

Characteristic MRI features of Baló-type lesions comprise circular layers of alternating signal intensity on T_1- or T_2-weighted (T_1w or T_2w, respectively) images.[1,2,6] Lesions are typically located within the cerebral white

matter, the basal ganglia, pons, cerebellum, and the spinal cord, while they usually spare the U-fibers.[1,2,7,8]

Clinical symptoms of BCS are described as (sub)acute onset of hemiparesis, hemianopia, or hemihypoesthesia, but also headache, encephalopathic symptoms, and seizures.[4,6,7] BCS patients treated with immunomodulatory and immunosuppressive drugs show recovery from symptoms and prolonged survival, similar to multiple sclerosis (MS).[1,4,6–8] In light of an overlap of neuropathological and clinical findings,[1,3,8,9] the question arises as to whether BCS is a rare variant of MS, a disease entity of its own, or a clinical and radiological phenotype comprising different disease entities. Ultrahigh-field MRI at 7 Tesla (7 T) benefits from high spatial resolution and enhanced susceptibility effects that improve the visualization, detection, and morphological description of inflammatory brain lesions.[10–13] More precisely, in T_2*w MRI, a central vessel can frequently be depicted within MS lesions, and the presence of a central vessel is believed to be typical for MS lesions.[10,11,13] Given the unresolved nosologic association of BCS with MS, we set out to investigate the similarities and differences of BCS and MS lesions via high spatial resolution 7 T MRI. We did so in a prospective observational study of 10 BCS patients and 10 MS patients to investigate whether ultrahigh field lesion characteristics that are considered typical of MS are also present in BCS patients. Moreover, we compared additional clinical and paraclinical findings in BCS and in MS patients, including the course of the disease (re-scan and telephone interview), and testing for autoantibodies against aquaporin-4 (AQP4), and myelin oligodendrocyte glycoprotein (MOG-IgG) that have been reported in patients with large or tumefactive brain lesions.[14–17]

Methods

Study participants

Ten BCS patients were prospectively recruited from the neuroimmunology outpatient clinics of the Experimental and Clinical Research Center and the NeuroCure Clinical Research Center at Charité – Universitätsmedizin Berlin. The patients had been referred to Charité for obtaining a second opinion. The study design is outlined and detailed in Figure 1. Inclusion criteria were age 18–65 years and diagnosis of BCS that was based on conventional MRI findings (at least two hyperintense areas separated by one hypo-/isointense rim on T_2w images)[1,3,8,18–20] and confirmed by histopathological analyses in three patients. The only exclusion criterion was contraindication to undergo 7 T MRI. For comparison, the 10 best-matching patients regarding disease duration, age, and sex with relapsing remitting MS (RRMS) for whom 7 T MRI scans were available were selected from the NeuroCure neuroimaging database as controls. The study was conducted in conformity with the Declaration of Helsinki and approved by the ethics committee of Charité – Universitätsmedizin Berlin. All participants provided written informed consent.

Clinical and paraclinical characterization

Medical records of the BCS patients were used to obtain data on the initial clinical presentation, disability measured through the Expanded Disability Status Scale (EDSS),[21] CSF oligoclonal bands, immunomodulatory treatment as well as disease duration. In addition, BCS patients underwent clinical examination and EDSS assessment at the time of 7 T MRI (±30 days). Disease duration was defined as time between first symptoms (onset) and 7 T MRI. The follow-up period started with the completion of the 7 T examination and ended with a telephone interview (Fig. 1). In order to investigate a possible association with neuromyelitis optica spectrum disorders or anti-MOG antibody-associated encephalomyelitis, serum samples from all 10 BCS patients were tested for serum AQP4- and MOG-IgG at the University Hospital Heidelberg[14] using a cell-based assay (CBA).[14] CBA employed human embryonic kidney 293 cells transfected with human full-length MOG as previously described[14]; nontransfected cells were used as control substrate.

MR imaging acquisition

Ultrahigh-field MR images of BCS and RRMS patients were acquired using a 7 T Siemens whole-body scanner (Magnetom, Siemens, Erlangen, Germany) and a 24-channel receiver head coil (Nova Medical, Wilmington, MA) equipped with a birdcage volume coil for transmission. The imaging protocol included a two-dimensional T_2*w fast low-angle shot sequence (T_2*w, FLASH, TE = 25 msec; TR = 1820 msec; spatial resolution = 0.5 × 0.5 × 2 mm^3, supratentorial coverage), a three-dimensional T_1-weighted magnetization-prepared rapid gradient echo sequence (T_1w, MPRAGE, TE = 2.98 msec; TR = 2300 msec; inversion time [TI] = 900 msec; spatial resolution = 1.0 × 1.0 × 1.0 mm^3, whole-brain coverage), a three-dimensional fluid-attenuated inversion recovery sequence (FLAIR, TE = 398 msec; TR = 8010 msec; TI = 2150 msec, spatial resolution = 1.0 × 1.0 × 1.0 mm^3), and a three-dimensional gradient echo flow-compensated susceptibility-weighted imaging sequence (SWI, TE = 14 msec, TR = 25 msec, flip angle = 12°; spatial resolution = 0.5 × 0.5 × 1.0 mm^3, supratentorial coverage) that yields magnitude, phase, and reconstructed SW images.

In addition, a very high-resolution 2D T_2*w FLASH sequence (TE = 25 msec; TR = 1820 msec; spatial

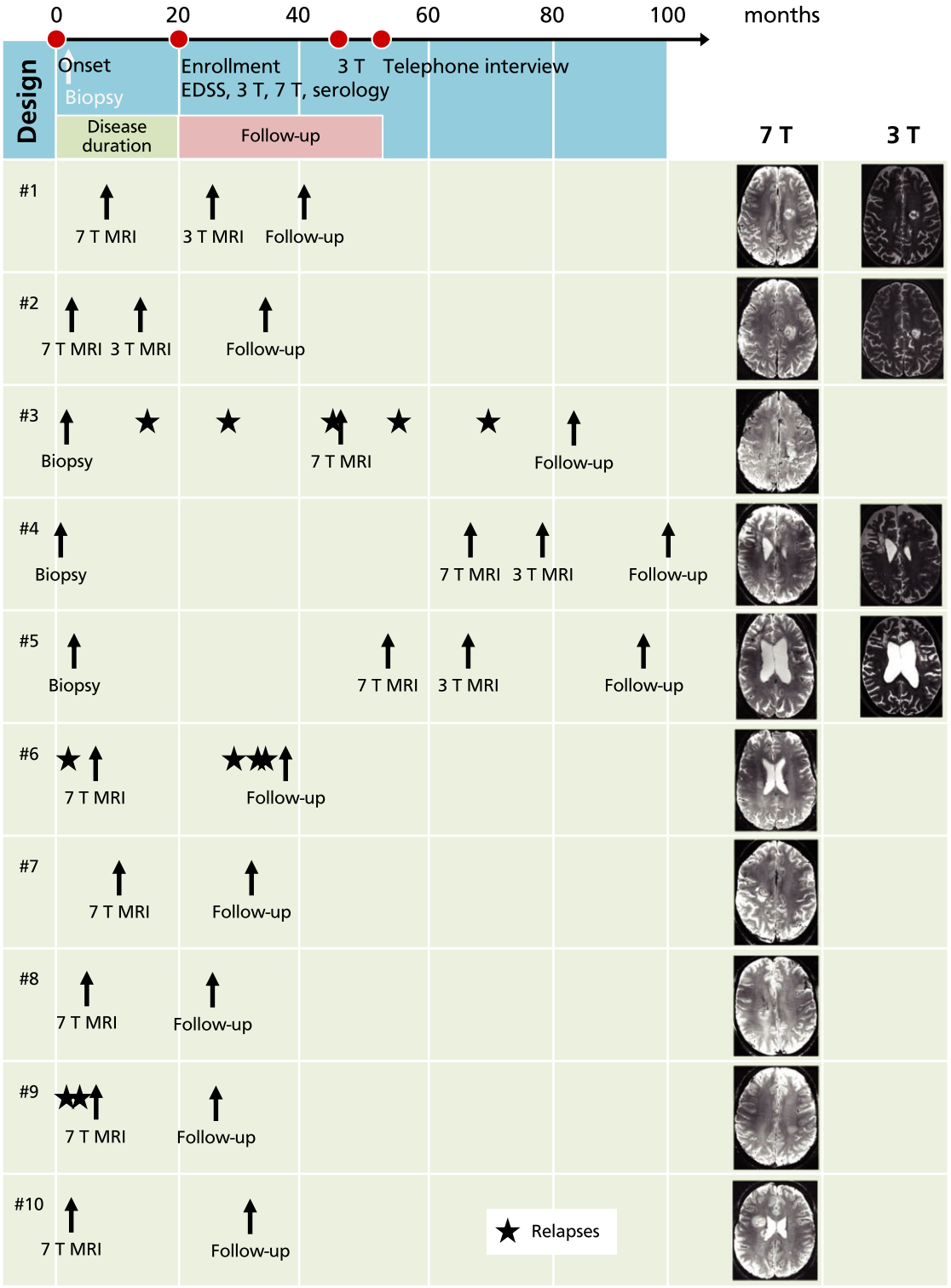

Figure 1. Overview. A timeline of the overall study design (top) is displayed in addition to clinical and paraclinical findings of all individual patients with Baló concentric sclerosis (bottom). The overall study design graphic represents mean time intervals between the single time points. Patients were recruited in the outpatient clinic of the Charité – Universitätsmedizin Berlin after the diagnosis of Baló concentric sclerosis. Three patients with Baló concentric sclerosis underwent biopsy and/or surgical resection prior to study enrollment. Two patients had relapses during the follow-up period (asterisks). 7 T, 7 Tesla MRI; 3 T, 3 Tesla MRI.

resolution = 0.2 × 0.2 × 2 mm^3) was done in nine patients with Baló-type lesions. For information on the 3 T MRI protocol please see Data S1.

Image analysis

The 7 T MR images were analyzed by two experienced investigators (Julia Wanner, Tim Sinnecker) who did not have any knowledge of clinical details (EDSS, age, sex) in consensus reading, using the OsiriX software package (OsiriX Foundation, Genève, Switzerland, version 3.8.1). BCS lesion morphology, including the existence of a central venous vessel, a T_2*w hypointense rim, and intralesional T_2*w signal alterations, was assessed in consensus reading. A central vein in a Baló-type lesion was defined as a vein that runs in equidistance to the border through the inner circle of a Baló-type lesion.

In addition, the number of additional non-Baló lesions in BCS patients was determined. Hereby, a brain lesion was defined as a hyperintense area of at least three voxels on FLAIR and T_2*w images. The "central vein sign" was assessed in these lesions according to NAIMS criteria in consensus reading.[22] In addition, the involvement of U-fibers, the existence of Dawson's fingers, and Barkhof criteria were assessed.[23]

The analysis of the 3 T MR images included the assessment of the MRI part (dissemination in space and time) of the 2010 MS diagnostic panel criteria,[24] based on 3 T MR image taken at the beginning of the study. The follow-up 3 T MRI images were analyzed with regard to newly developed lesions and whether a patient met positive MS diagnostic criteria.[24]

Statistical analysis

A Mann–Whitney *U*-test was used to detect differences between MS and BCS patients. $P < 0.05$ were considered statistically significant.

Results

Study participants

Ten patients with Baló-type lesions detected by MRI at disease onset were included (nine female). Mean age was 35.2 (SD = 7.9 years, range 27–49 years), and the mean disease duration – from disease onset to acquisition of the 7 T MR image – was 20.6 months (SD = 24.4 months, range 3–67 months). BCS patients presented with a median EDSS of 3.75 (range 2.0–4.0). The median clinical follow-up was 31.0 months (range 21–38 months).

As a control group, 10 patients with relapsing–remitting MS (RRMS) with comparable sex and age distribution and EDSS scores were included (nine female; mean ± SD age 31.7 ± 6.8 years, range 23–43 years, $P = 0.28$; mean ± SD disease duration 31.2 ± 34.3 months, range 2–113 months, $P = 0.53$; median EDSS 1.5, range 0–2.0). More clinical details of the BCS patients are presented in Table 1 and Figure 1.

Clinical findings in patients with Baló-type lesions

Hemiparesis and/or hemihypoesthesia were the most frequent symptoms at disease onset ($n = 7$) in BCS patients. Eight of 10 patients showed an acute onset of symptoms within hours to maximum symptom development, while all 10 MS patients exhibited a subacute onset within days to maximum symptom development. The majority of BCS patients ($n = 7$) had no further relapses until the end of observation, whereas three patients had relapses (Table 3). There was no difference in age ($P = 0.67$), gender ($P = 0.83$), disease duration ($P = 1$), and median duration until the follow-up examination ($P = 1$) between BCS patients with or without relapses. None of the BCS patients reported neurological symptoms prior to the symptomatic BCS lesion. All BCS patients received methylprednisolone pulse therapy as an acute relapse treatment at onset. In seven out of 10 patients, symptoms were mitigated during methylprednisolone pulse therapy (Table 1). Plasmapheresis was done in two patients. Symptoms in these two patients incompletely recovered during plasmapheresis. Cyclophosphamide cycles and immunoglobulin therapy was given to one patient and had no clinical effect. After the relapse therapy, treatment regimens of BCS patients comprised immunomodulation with glatiramer acetate ($n = 3$), interferon beta-1a ($n = 1$), dimethyl fumarate ($n = 3$), natalizumab ($n = 2$) as well as immunosuppression with cyclophosphamide and subsequently azathioprine ($n = 1$) (Table 1). Relapses during treatment are summarized in Table 3.

Lesion morphology of Baló-type lesions in 7 Tesla MRI

MR imaging findings are presented in Figure S1 and summarized in Table 2. Lesion morphology at the time of the 7 T MR imaging was partially concealed in three patients due to surgical resection or biopsy. MR imaging before biopsy or surgical resection is shown in Figure S2. All but the two partially resected Baló-type lesions had characteristic lesions with concentric rings on 7 T MR images (Fig. 2, Fig. S1). The rim thickness varied across subjects: Four patients had rather thick rims of more than 0.5 cm, and four patients had rims smaller than 0.5 cm (Fig. S3). In greater detail, T_2*w

Table 1. Characteristics of patients with Baló's concentric sclerosis at study onset.

ID	Age (years)	Sex	Disease duration (in months)	EDSS	Onset	Symptoms of presentation	Acute therapy	Months until initiation of DMT	Disease modifying therapy (DMT)	CSF white blood cells/μL (total)	OCB
#1	28	W	8	2.5	Stroke-like	Aphasia, hemihypesthesia (right side), vertigo, fatigue	Methyl-prednisolone 1 g for 4 days	19	Dimethyl fumarate	1	No
#2	27	M	3	2.5	Stroke-like	Hemiparesis (right side)	Methyl-prednisolone 1 g for 5 days and five times plasmapheresis	4	Dimethyl fumarate	12	Yes (Type 2)
#3	32	W	45	2.0	Stroke-like	Sensomotor hemiparesis (right side)	Methyl-prednisolone 1 g for 5 days	65	Natalizumab	8	Yes (Type 2)
#4	44	W	67	4.0	Stroke-like	Paresis of the left arm	Methyl-prednisolone 1 g for 5 days	2	Glatiramer acetate	13	Yes (Type 2)
#5	45	W	53	4.0	Subacute progressive (all symptoms)	Encephalopatic symptoms (cognitive deficits, social isolation)	Methyl-prednisolone 1 g for 5 days and immuneglobuline	4	Glatiramer acetate	4	Yes (Type 2)
#6	49	W	6	4.0	Stroke-like	Facial and hemiparesis, left side	Methyl-prednisolone 1 g for 5 days	1	Natalizumab	19	No
#7	33	W	10	4.0	Stroke-like	Hemiparesis, (left side), dysarthria	Methyl-prednisolone 1 g for 5 days, plasmapheresis and three cycles of cyclophosphamide	11	Azathioprine	2	Yes (Type 2)
#8	35	W	5	4.0	Stroke-like	Hemiparesis (left side)	Methyl-prednisolone 1 g for 5 days	1	Glatiramer acetate	>10	Yes (Type 2)
#9	31	W	6	2.5	Subacute progressive (all symptoms)	Prosopagnosia, vertigo, hemihypesthesia (right side)	Methyl-prednisolone 1 g for 2 days	4	Natalizumab	5	Yes (Type 2)
#10	28	W	3	3.5	Stroke-like	Hemiparesis (left side), dysarthria, fatigue	Methyl-prednisolone 1 g for 3 days	4	Interferon beta-1a	6	Yes (Type 2)

ID, identification number; EDSS, Expanded Disability Status Scale; Disease duration, time between onset, and 7 T intervention; OCB, oligoclonal bands; Oligoclonal bands Type 2, Oligoclonal IgG restricted to CSF.

and SWI hypointense rim-like structures were regularly observed at the border between T_2*w and FLAIR hyperintense areas ($n = 8$). These T_2*w and FLAIR hyperintense areas corresponded to T_1w hypointense lesion areas. In one Baló-type lesion, brain tissue in-between T_2w hyperintense rims layers was characterized by T_2*w and T_1w gray-scale intensity values similar to normal appearing white matter (Fig. S4) as reported previously.[25] In addition, lesions in four out of 10 BCS patients (patients #1, #4, #5, and #7) had an inhomogeneous intralesional T_2*w signal distribution, which is suggestive of microhemorrhages or small ectatic venous vessels within the lesions (Fig. 3). All Baló-type lesions ($n = 10$) had spatial contact to the lateral ventricles and the periventricular white matter preserving cortical areas or U-fibers.

Central veins within Baló-type lesions

A distinct venous vessel was clearly visible in the center of seven Baló-type lesions (Fig. 2), and not detectable in one Baló-type lesion. In two BCS patients, the central vein sign was not analyzable due to surgical resection.

Comparison between non-Baló lesions in BCS patients and RRMS controls

Next, we compared imaging findings between non-Baló lesions in the BCS group and brain lesions in the 10 matched RRMS patients.

In the BCS group, 97 non-Baló lesions were identified in eight of 10 patients (Table 2). In the RRMS control group, a total number of 204 lesions (median 5 ± 29 lesions per patient, range 1–93) were analyzed.

First, the existence of a central vein was analyzed in these lesions. In BCS, 36 of the 97 (37%) non-Baló lesions were encircled around a central vein that was visible on T_2*w images (Fig. 4). The median proportion of lesions with a central vein in additional non-Baló lesions per patient was 42% (range 0–100%). More specifically, four BCS patients were characterized by a proportion of at least 40% of lesions with a central vein (patients #2, #3, #9, #10). In two additional BCS patients (patients #1, #8) a clearly visible central vein was evident in one of three non-Baló lesions. The central vein sign was detectable in less than 40% of lesions and thus considered negative in BCS patient #6 (the proportion of lesions with a central vein was 24%). Patients #4 and #7 had no non-Baló lesions at all. In patient #5, a vein was found in the center of two of four lesions, but the lesions did not follow the course of the vein.

In the control group, nine of 10 RRMS patients had at least 40% or more lesions with a central vein (156 of 204 lesions [=77%], median 4.0 lesions per patient, range 0–77).

Second, U-fiber involvement and the existence of cortical lesions were assessed. Cortical lesions or involvement of U-fibers were absent in all BCS patients. By contrast, two RRMS patients exhibited cortical gray matter lesions (six of 204 lesions, 3%), and an involvement of U-fibers was present in four RRMS patients.

In addition, Dawson's finger-shaped lesions were found in three of 10 BCS patients (patients #1, #3, #8; Fig. 4), and eight of 10 RRMS patients.

Spinal cord MRI and follow up at 3 T

About nine BCS patients underwent standardized 3 T MRI within 6 weeks before or after the baseline 7 T scan. The 3 T scan included spinal cord MRI in four patients (Table 3). No spinal cord lesions were detected (Table 3).

Follow-up 3 T MRI was performed in four patients – after 12 months in patient #2, #4, #5, and after 18 months in patient #1 (Table 3). In these 4 patients, no new lesions were detected at follow-up.

Evaluation of MS diagnostic panel criteria in BCS patients

We investigated whether BCS patients fulfilled diagnosis of MS as defined by the 2010 MS diagnostic panel criteria.[24] At study baseline, four of 10 BCS patients fulfilled the 2010 MS diagnostic panel criteria (patient #1, #3, #6, and #9, Table 3). In particular, all four patients fulfilled the MRI criteria for dissemination in space. The MRI criteria for dissemination in time were positive in three patients (patients #1, #3, and #6). Clinical criteria for dissemination in time were positive in patients #3, #6, and #9.

During the follow-up period, two of the four BCS patients who met MS diagnostic criteria at baseline had further relapses (patients #3 and #6). By contrast, no new lesions or relapses were detectable in the BCS patients who were initially negative with respect to MS diagnostic criteria. In other words, none of these BCS patients met MS diagnostic criteria during follow-up.

One limitation is that the assessment of the 2010 MRI criteria for dissemination in time was not possible at baseline in one BCS patient because no contrast agent was given.

Histopathological findings in three BCS patients

Brain biopsy and/or surgical resection was done prior to this study in three BCS patients (Table 4). The biopsy

Table 2. MRI findings – lesion morphology and localization in BCS and MS.

ID	Lesion number (BCS: additional lesions to BCS)	Central vein (Baló lesions)	Central vein (non-Baló lesions)	Dawson's fingers	Barkhof criteria (brain MRI)	U-fiber involvement	Cortical lesions
BCS group							
BCS #1	3	Yes	1 (33%)	Yes	No	No	No
BCS #2	4	Yes	2 (50%)	No	No	No	No
BCS #3	11	No	9 (82%)	Yes	Yes	No	No
BCS #4	0	N/A	N/A	No	No	No	No
BCS #5	4	N/A	2 (50%)	No	No	No	No
BCS #6	62	Yes	14 (24%)	No	No	No	No
BCS #7	0	Yes	N/A	No	No	No	No
BCS #8	3	Yes	1 (33%)	Yes	No	No	No
BCS #9	8	Yes	4 (50%)	No	No	No	No
BCS #10	2	Yes	2 (100%)	No	No	No	No
RRMS control group							
RRMS #1	1	N/A	1	No	No	No	No
RRMS #2	2	N/A	2	Yes	No	No	No
RRMS #3	17	N/A	11	Yes	Yes	Yes	No
RRMS #4	36	N/A	22	Yes	Yes	Yes	No
RRMS #5	4	N/A	4	No	No	No	1
RRMS #6	40	N/A	33	Yes	Yes	Yes	5
RRMS #7	5	N/A	2	Yes	No	No	No
RRMS #8	1	N/A	1	Yes	No	No	No
RRMS #9	5	N/A	4	Yes	No	No	No
RRMS #10	93	N/A	77	Yes	Yes	Yes	No

BCS, Baló's concentric sclerosis; MRI, magnetic resonance imaging; MS, multiple sclerosis; ID, identification number; RRMS, relapsing–remitting MS; Barkhof criteria, >3/4 positive; Possible central vein was not detectable due to operation or biopsy (not applicable, n.a.).

decision was independently made by the treating center specialized in neurology. Specimens of all three BCS patients were characterized by demyelinating processes with almost complete loss of myelin. Furthermore, a predominately T-cell–driven perivascular lymphocyte infiltration ($n = 2$) as well as activated microglia ($n = 2$), astrogliosis with hypertrophic astrocytes ($n = 2$) and a reduction of axonal density ($n = 2$) were regularly observed within the lesion. While in one patient the oligodendrocytes had enlarged nuclei, oligodendrocytes were relatively well preserved in another. The axons in one patient were predominantly preserved. In one patient, astrocytes containing fragmented nuclei (Creutzfeldt–Peters cells) were found.

Biomarkers in patients with Baló-type lesions

Eight of 10 BCS patients had type 2 oligoclonal bands in CSF but not in serum indicative of intrathecal IgG synthesis (all three BCS patients with relapses; three of the four BCS patients with positive 2010 MS diagnostic criteria; Table 1).[26] None of the BCS patients had antibodies to AQP4 or MOG antibodies in serum.

Discussion

In this prospective ultrahigh-field MRI study we investigated lesion characteristics in 10 BCS patients in comparison to 10 typical RRMS patients without Baló-type lesions. A central intralesional vein – characteristic for MS lesions – was detectable within the majority of Baló-type lesions, and a periventricular lesion distribution was common in both disease types. In contrast to RRMS controls, lesions in the cortical gray matter and subcortical U-fibers were absent in all patients with BCS. Some lesions in BCS patients were characterized by signs of peripheral ectatic veins. In alignment with our in vivo results, previous ex vivo investigations indicated that the inflammation expands from a central venule into the surrounding white matter in both MS- and BCS-derived lesions.[6,27] In contrast to MS, alternating patterns of demyelination and preservation seem to proceed periodically in BCS, causing the characteristic large multilayer lesions.[7,19,20,28–30] However, the pathophysiologic underpinnings of this lesion pattern are currently not well understood. Several mechanisms have been suggested, including alternating gradients of proinflammatory and anti-inflammatory agents, oxidative stress resulting in

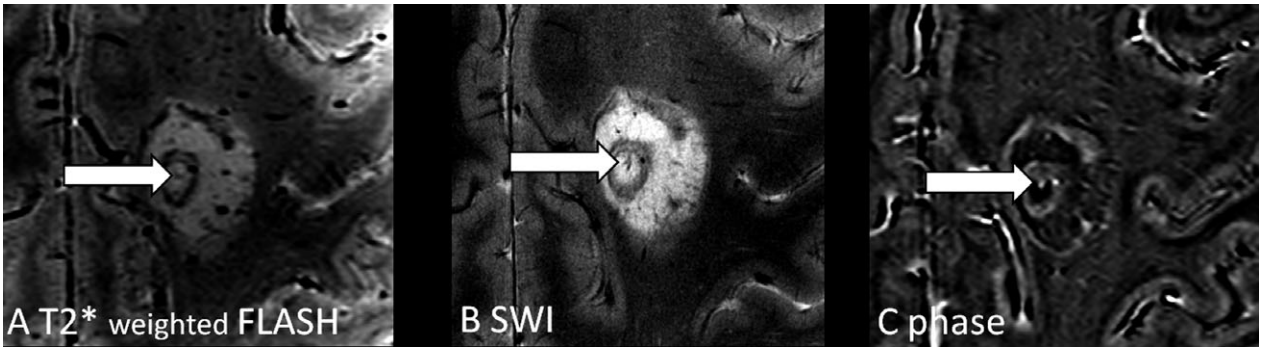

Figure 2. Central intralesional vein in Baló concentric sclerosis. A distinct venous vessel is clearly visible within the center of the inner ring of one exemplary Baló-type lesion on 7 T, T_2*w (A), SWI (B) and MR phase images (C). 7 T, 7 Tesla; T_2*w, two-dimensional T_2*-weighted fast low-angle shot (FLASH); SWI, three-dimensional gradient echo flow-compensated susceptibility-weighted imaging.

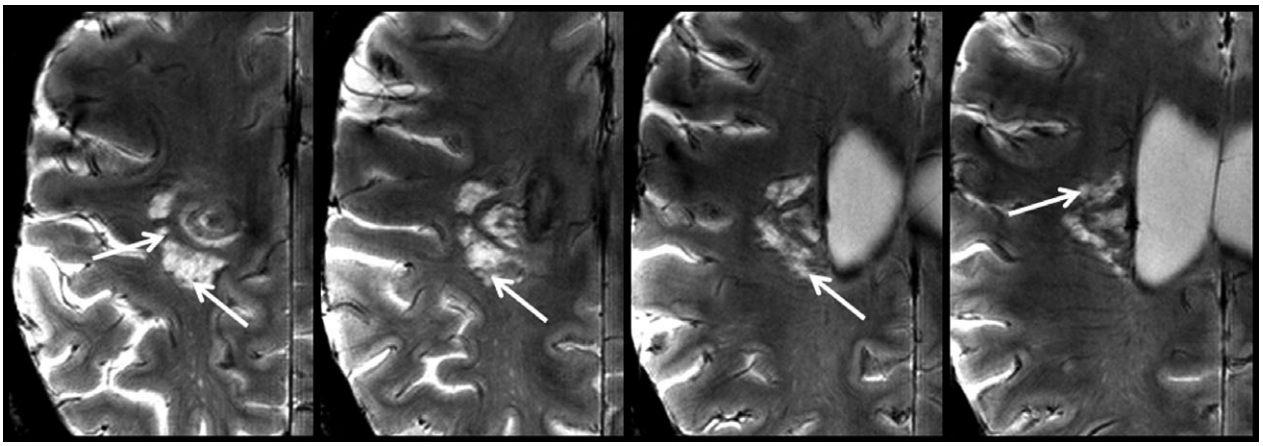

Figure 3. Inhomogeneous intralesional T_2*w signal distribution within an exemplary Baló-type lesion. 7 T T_2*w images of one exemplary lesion (patient #7) are presented demonstrating T_2* hypointense structures (arrows) within the lesion. These signal alterations potentially indicate microhemorrhages or small ectatic venous vessels. 7 T, 7 Tesla; T_2*w, two-dimensional T_2*-weighted fast low-angle shot (FLASH).

hypoxia-like tissue injury with a combination of protective and damaging factors, astrocytopathy as well as loss of aquaporin 4 and connexin 43 which causes oligodendrocytopathy.[1,2,19,30,31]

In this study, an inhomogeneous intralesional T_2*w signal intensity was observed in four of 10 Baló-type lesions, which may be related to microhemorrhages or small ectatic venous vessels within the lesions. Similar findings including microhemorrhages and ectatic veins in T_2w hyperintense regions of a Baló-type lesion were previously described in a 7 T case report.[32] The visibility of venous structures on T_2*w images of 7 T is dependent on the degree of deoxygenation of the venous blood, since only desoxyhemoglobine causes signal loss as a consequence of the magnetic susceptibility effects.[12] In line with previous MR spectroscopy and diffusion-weighted MRI studies,[7,32] these imaging findings may reflect alterations in oxygen demand and are in line with the hypothesis of hypoxia-induced tissue degeneration during Baló-type lesion formation. In addition, a potential overlap of BCS with other atypical inflammatory demyelinating syndromes like tumefactive demyelination as well as MOG-IgG- or AQP4-IgG-associated brain damage has been proposed.[3,33,34] In our study, Creutzfeldt–Peters cells, a histopathological feature of tumefactive demyelination, were detectable in one biopsy.[3,33] AQP4-IgG and MOG-IgG were negative in all BCS patients, suggesting that these antibodies do not play a key role in the pathogenesis of BCS.

Aside from these pathophysiological considerations another key aspect of this study was to compare clinical and paraclinical findings between patients with MS and BCS. Similar to MS patients, our BCS patients often exhibited positive oligoclonal bands ($n = 8$), Dawson's fingers ($n = 3$), and a visible central vein in 36 of 97 non-Baló lesions. While lesions that appeared to be typical MS lesions were also found in previous reports,[4,5,9,20]

Figure 4. MS-typical lesions in Baló concentric sclerosis. A T_2*w image is displayed showing multiple MS-typical lesions (circle) with a central vein in addition to a single but prominent Baló-type lesion (arrow). T_2*w, two-dimensional T_2*-weighted fast low-angle shot (FLASH); MS, multiple sclerosis.

oligoclonal bands have been reported only in approximately two-thirds of BCS patients.[5–7,35] Wallner-Blazek et al. assumed the coexistence of MS-type lesions in patients with atypical demyelinating lesions, including Baló-type lesions, as an indicator of future disease activity.[9]

Table 3. 3 T MRI and clinical follow-up in patients with Baló concentric sclerosis.

	Baseline (MRI)					Follow-up (MRI)			Follow-up (clinical)		Follow-up
ID	DiS	DiT	Contrast enhancement	Spinal cord lesions	MS diagnosis (MRI part only)[24]	New lesions	Spinal lesions	MS diagnosis (MRI part only)[24]	Follow-up (months)	Disease course until end of follow-up	MS diagnosis (clinical and MRI part combined)
#1	Yes	Yes	Asymptomatic	N/A	Yes	No	N/A	Yes	34	No further relapses	Yes
#2	Yes	No	No	N/A	No	No	N/A	No	33	No further relapses	No
#3	Yes	Yes	Yes	No	Yes	N/A	N/A	N/A	38	Five relapses in total, one relapse under therapy	Yes
#4	Yes	No	No	N/A	No	No	N/A	No	33	No further relapses	No
#5	Yes	No	Symptomatic	No	No	No	No	No	31	No further relapses	No
#6	Yes	Yes	Asymptomatic	N/A	Yes	N/A	N/A	N/A	31	Four relapses in total, three relapses under therapy	Yes
#7	No	No	No	No	No	N/A	N/A	N/A	22	No further relapses	No
#8	Yes	No	No	No	No	N/A	N/A	N/A	21	No further relapses	No
#9	Yes	No	N/A	N/A	N/A	N/A	N/A	N/A	21	Two relapses, no relapse under therapy	Yes
#10[1]	Yes	No	Symptomatic	N/A	No	N/A	N/A	N/A	29	No further relapses	No

ID, identification number; MRI, magnetic resonance imaging; N/A, not available; DiS, dissemination in space; DiT, dissemination in time; symptomatic, contrast enhancement correlates with the clinical presentation; asymptomatic, contrast enhancement does not correlate with the clinical presentation.

[1]Baseline data of patient ID 10 were derived from 7 T MRI. Follow-up: time between 7 T intervention and telephone interview.

Table 4. Histopathological findings in patients with Baló concentric sclerosis.

ID	Demyelination	Histological characteristics	Cell infiltration
#3	Sharply limited, inactive demyelination	Astrogliosis Hypertrophic astrocytes Activated microglia Oligodendrocytes with hypertrophic nuclei in the outlying areas Reduced axons	T-cell dominating and diffuse infiltration Plenty of macrophages
#4	Limited demyelination	Astroctopathy with two or more nuclei Astrocytopathy surrounding the lesion Axons relatively well-preserved, occasionally hypertrophic	T-cells perivascular
#5	Demyelination inside the lesion	Astrogliosis Hypertrophic astrocytes Creutzfeldt–Peters cells Activated microglia Relatively well-preserved oligodendrocytes inside the lesion Reduced axons	Lymphocytes Plasma cells Foamy macrophages

ID, identification number.

On this background, one might speculate that BCS is a heterogeneous disease of which one subgroup shares common features with MS (oligoclonal bands, MS-type lesions, relapses) while a different subgroup is characterized by a different etiopathogenesis. Our data is not conclusive on this issue: On one hand, three BCS patients met the diagnostic criteria for MS at the onset of the study, and two of these had further relapses. In addition, all three BCS patients with a relapsing–remitting disease course indeed exhibited additional non-Baló lesions with a central vein, and two displayed positive oligoclonal bands. On the other hand, we also observed similar findings in the group without further relapses during the period of observation, and a recent systematic review did not describe differences between BCS patients with and without oligoclonal bands.[35] Thus, a longer follow-up is needed to ultimately determine the prognostic relevance of a positive central vein sign, Dawson's fingers, or oligoclonal bands in BCS.

One clear difference between BCS and RRMS controls, however, was that in our study – in line with the literature (Table 5)[4–7,18] – the majority of BCS patients showed a stroke-like onset with relatively severe symptoms like hemiparesis and hemihypesthesia.

Our study is not free from limitations. The small sample size and the short follow-up period in some patients

Table 5. Review of the literature: time course of development of symptoms.

References	Acute onset	Subacute onset
Karaarslan et al.[6]	5 Baló concentric sclerosis patients with an acute onset	
Mowry et al.[7,8]	1 Baló concentric sclerosis patient with a stroke-like onset	
Wang et al.[4]	6 Baló concentric sclerosis patients with an acute onset	1 Baló concentric sclerosis patient with progressive clinical manifestation for a week
Purohit et al.[5]	1 Baló concentric sclerosis patient with an acute onset	
Chen et al.[18]	2 Baló concentric sclerosis patients with acute onset 15/20 Baló concentric sclerosis patients	4 Baló concentric sclerosis patients with a subacute onset 5/20 Baló concentric sclerosis patients

complicate the investigation of potential prognostic MR biomarkers. Blinding to the BCS diagnosis was obviously not fully achievable during MRI analysis, given the characteristic brain lesions in BCS. Finally, various treatment regimens most likely influenced clinical disease courses.

In summary, this is the first investigation of BCS patients using ultrahigh-field MRI in a prospective observational study. We observed differences between Baló patients and patients with RRMS, for instance, regarding lesion location, involvement of cortical gray matter and intralesional T_2*w signal inhomogeneities. Nevertheless, a central vein and Dawson's fingers, which are both typical of MS, were also present in some BCS patients. This suggests that both diseases share at least some pathophysiological commonalities. Although further prospective studies are needed, our investigations show that BCS is not necessarily a disease with a devastating prognosis. Indeed, more than two-thirds of the BCS patients included in our study had a clinically stable disease course without further relapses during the time span that we covered.

Acknowledgments

We thank our colleagues Antje Els, Cynthia Kraut, Susan Pikol, Gritt Stoffels, Ivonne Hinz, Timm Oberwahrenbrock, and Edzard Wiener for their great support. S. J. and B. W. are grateful to Anna Eschlbeck and the Nikon Imaging Center at the University of Heidelberg for excellent technical support and thank the Dietmar-Hopp-Stiftung for financially supporting research on the role of AQP4-IgG and MOG-IgG in the pathogenesis of demyelinating diseases of the CNS.

Declaration of Conflicts of Interest

Janina R. Behrens received travel funding from Biogen Idec, Bayer, Novartis, and Teva and speaker fees from Novartis. Julia Wanner and Lennard Ostendorf have no potential conflict of interest. Joseph Kuchling received conference registration fees from Biogen and financial research support from Krankheitsbezogenes Kompetenznetzwerk Multiple Sklerose (KKNMS), not related to this work. Lutz Harms received travel funding and/or speaker fees from Biogen Idec, Bayer, Grifols, HealthCare, Merck Serono, Teva and served on the scientific advisory board for Roche, Biogen, Sanofi/Genzyme, and Novartis. Klemens Ruprecht served on the scientific advisory boards for Sanofi-Aventis/Genzyme, Novartis, Roch,; received travel funding and/or speaker fees from Bayer HealthCare, Biogen Idec, Merck Serono, Sanofi-Aventis/Genzyme, Teva Pharmaceuticals, Novartis, and the Guthy Jackson Charitable Foundation, is an associate editor for PLOS ONE, received publishing royalties from Elsevier, and received research support from Novartis and the German Ministry of Education and Research. Thoralf Niendorf received travel funding and/or speaker fees from Siemens Healthcare; is founder and CEO of MRI TOOLS GmbH, and received research support from Siemens Healthcare and the Helmholtz Alliance ICEMED. Sven Jarius reports no conflicts of interest. Brigitte Wildemann has received research grants, speaker fees, and travel grants from Merck Serono, Biogen, Teva, Novartis, Sanofi Genzyme, Bayer Healthcare, Biotest, and the Dietmar Hopp Foundation. René M. Gieß received nonfinancial support from Novartis AG and Merck KGaA for travel and congress attendance. Judith Bellmann-Strobl received travel funding and/or speaker fees from Bayer Healthcare, Sanofi-Aventis/Genzyme, and Teva Pharmaceuticals. Friedemann Paul is on the steering committees for Novartis and MedImmune; received speaker fees and travel funding from Bayer, Novartis, Biogen Idec, Teva, Sanofi-Aventis/Genzyme, and Merck Serono, is an academic editor for PLOS ONE; is an associate editor for Neurology: Neuroimmunology & Neuroinflammation, has consulted for Sanofi-Aventis/Genzyme, Biogen Idec, and MedImmune, and received research support from Bayer, Novartis, Biogen Idec, Teva, Sanofi-Aventis/Genzyme, Merck Serono, German Research Council, Werth Stiftung of the City of Cologne, German Ministry of Education and Research, Arthur Arnstein Stiftung Berlin, EU FP7 Framework Program, Guthy Jackson Charitable Foundation, and National Multiple Sclerosis Society of the USA. Jens Wuerfel is CEO of MIAC AG, Switzerland; has served on advisory boards for Biogen, Genzyme, Novartis; received

speaker honoria from Byer, Novartis, Teva and Biogen. Tim Sinnecker received travel funding from Bayer, Teva, Novartis, Genzyme, Roche and Actelion and is employee at the MIAC AG, Switzerland.

References

1. Hardy TA, Miller DH. Baló's concentric sclerosis. Lancet Neurol 2014;13:740–746.
2. Kira J. Astrocytopathy in Balo's disease. Mult Scler 2011;17:771–779.
3. Hardy TA, Tobin WO, Lucchinetti CF. Exploring the overlap between multiple sclerosis, tumefactive demyelination and Baló's concentric sclerosis. Mult Scler 2016;22:986–992.
4. Wang C, Zhang K-N, Wu X-M, et al. Baló's disease showing benign clinical course and co-existence with multiple sclerosis-like lesions in Chinese. Mult Scler 2008;14:418–424.
5. Purohit B, Ganewatte E, Schreiner B, Kollias S. Balo's concentric sclerosis with acute presentation and co-existing multiple sclerosis-typical lesions on MRI. Case Rep Neurol 2015;7:44–50.
6. Karaarslan E, Altintas A, Senol U, et al. Baló's concentric sclerosis: clinical and radiologic features of five cases. AJNR Am J Neuroradiol 2001;22:1362–1367.
7. Mowry EM, Woo JH, Ances BM. Baló's concentric sclerosis presenting as a stroke-like syndrome. Nat Clin Pract Neurol 2007;3:349–354.
8. Mowry EM, Woo JH, Ances BM. Technology insight: can neuroimaging provide insights into the role of ischemia in Baló's concentric sclerosis? Nat Clin Pract Neurol 2007;3:341–348.
9. Wallner-Blazek M, Rovira A, Fillipp M, et al. Atypical idiopathic inflammatory demyelinating lesions: prognostic implications and relation to multiple sclerosis. J Neurol 2013;260:2016–2022.
10. Mistry N, Dixon J, Tallantyre E, et al. Central veins in brain lesions visualized with high-field magnetic resonance imaging: a pathologically specific diagnostic biomarker for inflammatory demyelination in the brain. JAMA Neurol 2013;70:623–628.
11. Kuchling J, Ramien C, Bozin I, et al. Identical lesion morphology in primary progressive and relapsing-remitting MS—an ultrahigh field MRI study. Mult Scler 2014;20:1866–1871.
12. Sinnecker T, Bozin I, Dörr J, et al. Periventricular venous density in multiple sclerosis is inversely associated with T2 lesion count: a 7 Tesla MRI study. Mult Scler 2013;19:316–325.
13. Sinnecker T, Kuchling J, Dusek P, et al. Ultrahigh field MRI in clinical neuroimmunology: a potential contribution to improved diagnostics and personalised disease management. EPMA J 2015;6:16.
14. Jarius S, Probst C, Borowski K, et al. Standardized method for the detection of antibodies to aquaporin-4 based on a highly sensitive immunofluorescence assay employing recombinant target antigen. J Neurol Sci 2010;291:52–56.
15. Kim HJ, Paul F, Lana-Peixoto MA, et al. MRI characteristics of neuromyelitis optica spectrum disorder: an international update. Neurology 2015;84:1165–1173.
16. Jarius S, Ruprecht K, Kleiter I, et al. MOG-IgG in NMO and related disorders: a multicenter study of 50 patients. Part 1: frequency, syndrome specificity, influence of disease activity, long-term course, association with AQP4-IgG, and origin. J Neuroinflammation 2016;13:279.
17. Zamvil SS, Slavin AJ. Does MOG Ig-positive AQP4-seronegative opticospinal inflammatory disease justify a diagnosis of NMO spectrum disorder? Neurol Neuroimmunol Neuroinflamm 2015;2:e62.
18. Chen F, Liu T, Li J, et al. Eccentric development of Balo's concentric sclerosis: detected by magnetic resonance diffusion-weighted imaging and magnetic resonance spectroscopy. Int J Neurosci 2015;125:433–440.
19. Stadelmann C, Ludwin S, Tabira T, et al. Tissue preconditioning may explain concentric lesions in Baló's type of multiple sclerosis. Brain 2005;128(Pt 5):979–987.
20. Koelblinger C, Fruehwald-Pallamar J, Kubin K, et al. Atypical idiopathic inflammatory demyelinating lesions (IIDL): conventional and diffusion-weighted MR imaging (DWI) findings in 42 cases. Eur J Radiol 2013;82:1996–2004.
21. Kurtzke JF. Rating neurologic impairment in multiple sclerosis: an expanded disability status scale (EDSS). Neurology 1983;33:1444–1452.
22. Sati P, Oh J, Constable RT, et al. The central vein sign and its clinical evaluation for the diagnosis of multiple sclerosis: a consensus statement from the North American Imaging in Multiple Sclerosis Cooperative. Nat Rev Neurol 2016;12:714–722.
23. Barkhof F, Filippi M, Miller DH, et al. Comparison of MRI criteria at first presentation to predict conversion to clinically definite multiple sclerosis. Brain 1997;120(Pt 11):2059–2069.
24. Polman CH, Reingold SC, Banwell B, et al. Diagnostic criteria for multiple sclerosis: 2010 revisions to the McDonald criteria. Ann Neurol 2011;69:292–302.
25. Darke ME, Bahador FM, Miller DC, et al. Baló's concentric sclerosis: imaging findings and pathological correlation. J Radiol Case Rep 2013;7:1–8.
26. Reiber H, Peter JB. Cerebrospinal fluid analysis: disease-related data patterns and evaluation programs. J Neurol Sci 2001;184:101–122.
27. Moore GR, Berry K, Oger JJ, et al. Baló's concentric sclerosis: surviving normal myelin in a patient with a relapsing-remitting dinical course. Mult Scler 2001;7:375–382.
28. Popescu BFG, Lucchinetti CF. Pathology of demyelinating diseases. Annu Rev Pathol Mech Dis 2012;7:185–217.

29. Khonsari RH, Calvez V. The origins of concentric demyelination: self-organization in the human brain. PLoS One 2007;2:e150.
30. Takai Y, Misu T, Nishiyama S, et al. Hypoxia-like tissue injury and glial response contribute to Balo concentric lesion development. Neurology 2016;87:2000–2005.
31. Matsuoka T, Suzuki SO, Iwaki T, et al. Aquaporin-4 astrocytopathy in Baló's disease. Acta Neuropathol 2010;120:651–660.
32. Berghoff M, Schlamann MU, Maderwald S, et al. 7 Tesla MRI demonstrates vascular pathology in Balo's concentric sclerosis. Mult Scler 2013;19:120–122.
33. Lucchinetti CF, Gavrilova RH, Metz I, et al. Clinical and radiographic spectrum of pathologically confirmed tumefactive multiple sclerosis. Brain 2008;131:1759–1775.
34. Hardy TA, Reddel SW, Barnett MH, et al. Atypical inflammatory demyelinating syndromes of the CNS. Lancet Neurol 2016;15:967–981.
35. Jarius S, Würthwein C, Behrens JR, et al. Baló's concentric sclerosis is immunologically distinct from multiple sclerosis: results from retrospective analysis of almost 150 lumbar punctures. J Neuroinflammation 2018;15:22.

Supporting Information

Additional Supporting Information may be found online in the supporting information section at the end of the article:

Figure S1. 7 T MR images at study onset. 7 T T_2*w images acquired at study onset of all patients with Baló concentric sclerosis are presented. Each Baló-type lesion is framed. BCS patients who underwent a biopsy are marked with *. 7 T, 7 Tesla; T_2*w, two-dimensional T_2*-weighted fast low-angle shot (FLASH).

Figure S2. MR images prior to surgical resection or biopsy. The figure illustrates MR images that were acquired prior to biopsy or surgical resection showing contrast-enhancing Baló-type lesions in all three patients (patients #3, #4, and #5). Key: (A) fluid-attenuated inversion recovery (FLAIR) images; (B) T_1w contrast-enhanced images.

Figure S3. Lesion morphology of two exemplary Baló-type lesions. While lesion (A) is characterized by rather thin rims, lesion (B) exhibits a single thicker outer rim. The relevance of such different lesion morphologies is unknown yet. Please note the biopsy area in (A) (asterisk).

Figure S4. Intralesional T_2*w and T_1w gray-scale values of Baló-type lesions. T_2*w images (A and C) and T_1w images (B and D) of two patients with Baló-type lesions are displayed. In general, Baló-type lesions were characterized by alternating layers of T_2* hyperintense and hypointense layers. Hereby, T_2*w hyperintense areas usually correspond to strongly T_1w hypointense areas (A and B). In one patient (C and D), brain tissue in-between T_2w hyperintense rims appeared preserved (arrow in C and D), given that it was characterized by T_2*w and T_1w gray-scale intensity values similar to normal appearing white matter. T_2*w, two-dimensional T_2*-weighted fast low-angle shot (FLASH); T_1w, three-dimensional T_1-weighted magnetization prepared rapid gradient echo (MPRAGE).

Data S1. MR imaging acquisition of 3 T MRI sequences. The MR imaging acquisition of the 3 T MRI sequences (MPRAGE, T_2-weighted images and FLAIR) are shown. 3 T, 3-Tesla MRI; MPRAGE, three-dimensional T_1-weighted magnetization prepared rapid gradient echo; FLAIR, fluid-attenuated inversion recovery images.

